



Iron dynamics and isotope fractionation in soil and rice during 2000 years of rice cultivation

Bei Wu · Xiangtian Meng · Huaiying Yao ·
Wulf Amelung

Received: 28 August 2023 / Accepted: 12 October 2023 / Published online: 25 October 2023
© The Author(s) 2023

Abstract

Background and aims Paddy management results in frequent redox cycles of the soil and thus changes in the terrestrial iron (Fe) cycle. We intended to test that the increasing duration of paddy management and the increasing frequency of soil redox cycles leave their fingerprint on Fe isotope composition of paddy systems, which could subsequently be used to deduce the origin of rice plants as related to the extent of past soil paddy management.

Methods We sampled soil and rice plants of a paddy chronosequence in China with rice cultivation history up to 2000 years and determined the changes of soil

Fe pools and Fe isotope composition of the soil and rice plants.

Results Prolonged paddy management reduced Fe concentrations in submerged topsoil leading to an enrichment of heavy Fe isotopes, with the $\delta^{56}\text{Fe}$ values 0.12‰ heavier than the parent material after 2000 years. Particularly, Fe oxides were lost quickly, while exchangeable and organic-associated Fe continuously accumulated during paddy management and played an increasing role in the plant-available Fe pool in the topsoil. The Fe content in rice also increased with paddy age, while its Fe isotope composition did not reflect that of paddy soil but resembled that of the Fe plaques on the roots.

Conclusion Prolonged rice cropping altered the biological contribution in the terrestrial Fe cycle. However, while soil Fe pools that are closely linked with biological activities were affected rather quickly, the

Responsible Editor: Wolfgang Wilcke.

Supplementary Information The online version contains supplementary material available at <https://doi.org/10.1007/s11104-023-06352-5>.

B. Wu (✉) · W. Amelung
Institute of Bio- and Geosciences: Agrosphere (IBG-3),
Forschungszentrum Jülich GmbH (FZJ), Jülich, Germany
e-mail: b.wu@fz-juelich.de

X. Meng · H. Yao
Ningbo Observation and Research Station, Institute
of Urban Environment (NUEORS), Chinese Academy
of Sciences (CAS), Ningbo, China

X. Meng
College of Natural Resources and Environment, Northwest
Agriculture and Forestry University, Yangling, China

H. Yao
School of Environmental Ecology and Biological
Engineering, Wuhan Institute of Technology, Wuhan,
China

W. Amelung
Institute of Crop Science and Resource Conservation
(INRES), Universität Bonn, Bonn, Germany

changes in the whole soil Fe system were detectable only after a millennium of paddy management.

Keywords Iron isotope composition · Paddy chronosequence · Rice · Iron uptake · Terrestrial iron cycle

Introduction

Paddy soils feed half of the population on Earth with its rice products. The paddy management includes puddling, flooding of soil, and drainage, and thus results in redox potential oscillations and intensified cycling of redox-sensitive elements, such as of iron (Fe). Along with the switch of active microbial community structures from aerobic to anaerobic consumption of organic matter upon flooding, ferric (Fe(III)) species in soil, among others (such as manganese of quadrivalence (Mn(IV))), replace molecular oxygen (O₂) as the electron acceptor. The reductive dissolution of Fe(III) minerals is mediated by dissimilatory Fe reducing (DIR) bacteria (Lovley et al. 2004). The reduced Fe(II) is dissolved in soil water at pH 7 when the reducing potential is lower than 100 mV (Kögel-Knabner et al. 2010). As a consequence, soil water of flooded paddy fields is enriched in Fe(II) (Fe²⁺), which can be leached to deeper soil horizons and in other directions. Successive re-precipitation in depth results in the formation of an Fe-rich illuvial horizon that is often diagnostic for paddy fields with long-term rice cultivation (Cheng et al. 2009). The Fe in the illuvial horizon often shows zonation of brownish color, rich in Fe oxides.

Changes in the dynamics of Fe can be assumed to be associated with Fe isotope fractionation, as redox reactions of Fe and related dissolution and precipitation result in isotopically different Fe-containing reactants and products (Wu et al. 2019). Some of the largest Fe isotope fractionations occur between reduced and oxidized Fe forms, amounting for up to 1.4 to 2.9 delta units ($\delta^{56}\text{Fe}$, ‰, Johnson and Beard 2006). Because of this fractionation, oxidized Fe species are usually enriched in heavy Fe isotopes relative to their reduced counterparts (Wu et al. 2019). Regarding paddy fields, this isotope fractionation means that soil water enriched in Fe²⁺ is isotopically lighter than the Fe(III)-containing minerals, from which Fe²⁺ is dissolved or where the oxidized Fe precipitates. In this

sense, eluviation of Fe²⁺ and subsequent illuviation of Fe(III) should also result in differences in Fe isotope composition among soil horizons. Indeed, enhanced variation of Fe isotope composition was observed in paddy soil profiles, as a result of the preferential removal of isotopically light Fe (Huang et al. 2018).

In addition to redox oscillation on the level of soil horizons, there are microscale redox potential gradients in the rhizosphere of rice plants (Kögel-Knabner et al. 2010). Like many other aquatic and wetland plants, rice roots form aerenchyma and release O₂ to the root surface, e.g., helping alleviate the toxicity of abundant Fe²⁺ through oxidation (Becker and Asch 2005). As a result, Fe²⁺ in soil water is precipitated on the root surface as so-called Fe plaques. These Fe plaques are composed of both crystalline and short-range-ordered Fe oxide phases. Using synchrotron radiation X-ray absorption spectroscopy, Amaral et al. (2017) revealed that Fe in the plaques of rice roots was mainly composed of ferrihydrite, goethite, and lepidocrocite, with different magnitudes among cultivars and soil amendments.

Rice is a strategy II plant, capable of releasing phytosiderophores (PS) that chelate Fe(III) in the rhizosphere. The Fe(III)–PS complexes will be then imported by specific plasmalemma transporter proteins (e.g., Takagi et al. 1984). On the other hand, rice also has the ferrous transporter OsIRT1, which allows the crop to directly absorb Fe(II) ions from the soil water (Kobayashi and Nishizawa 2012) in addition to a PS-mediated Fe(III) transport system (Buglio et al. 2002). In other words, rice can take up Fe as Fe(III)-PS and Fe(II) ions (Ishimaru et al. 2006). Moreover, Ishimaru et al. (2006) proposed that rice plants directly absorb free Fe²⁺ via OsIRT1 and OsIRT2 transporters in a Fe-rich growth media such as a paddy soil, where Fe²⁺ is readily available. A paddy field study by Garnier et al. (2017) revealed a high enrichment of heavy Fe isotopes in rice roots relative to the plant-available Fe in the soil solution, suggesting that Fe was taken from the isotopically heavy Fe plaques rather than from the isotopically light Fe²⁺ in soil water. However, as Fe isotope fractionation also occurs during translocation from roots to shoots, the Fe isotope composition of plant roots cannot be used alone to deduce the isotope fractionation during uptake (Wiggenhauser et al. 2022). In this regard, the heavy isotope signature of rice roots shown by Garnier et al. (2017) can also be resulted

from in-plant translocation and transformation, as the aboveground organs exhibited light Fe isotope composition. On the other hand, by using an isotope mass balance approach, Chen et al. (2021) calculated respective contributions of paddy soil and the Fe plaques to the Fe in their rice plants, leading to their conclusion that about 70% of Fe in rice came from the soil. To this end, the contribution of Fe plaques to rice nutrition is thus still unclear. Assessing Fe isotope composition in whole rice plants, rhizosphere, as well as paddy soils of different duration of paddy use, however, may highlight the underlying processes, and to what degree they might have changed in the history of paddy management.

In the present study, we took advantage of a paddy chronosequence with rice cultivation history up to 2000 years (Kalbitz et al. 2013; Kölbl et al. 2014; Roth et al. 2011) to investigate 1) whether and to which degree changes in Fe concentration and Fe isotope composition of the submerged paddy topsoil can be scaled to land-use ages, and 2) whether and to which degree the Fe isotope composition of rice plants reflects that of Fe plaques and that of soil in relation to the duration of paddy soil management. In this regard, we intended to provide insight on how prolonged agricultural practices such as rice cropping would alter the terrestrial Fe cycle.

Materials and methods

Study site

The studied sites are located in a land reclamation area in the Bay of Hangzhou near the City of Cixi, Zhejiang Province, China, including a paddy chronosequence, a tidal wetland soil and adjacent cultivated non-paddy upland soils, which share the same Yangtze River sediments as parent material. According to the Edit Committee of Chorography of Cixi County (Wang 2004), rice cultivation has a history of up to 2000 years following successive dyke constructions. Upland soils of up to 700 years can be dated in adjacent areas to paddy, as non-paddy practices were not documented before. The reclamation for crop land-use continues even nowadays. During our sampling campaign in 2018, we found a newly constructed dyke behind which a paddy field had been established less than 5 years ago (denoted as P5 in the present

study). Annual precipitation in the region averages 1325 mm with a maximum between April and October, and the mean annual temperature is 16.3 °C (Cheng et al. 2009). The dominant clay mineral of the soil is illite (Wissing et al. 2014). The soils are characterized as Cambisols for non-paddy and younger paddy soils and Hydragric Anthrosols for paddy older than 100 years (Cheng et al. 2009). The soil texture varies between loam, silt loam and silt clay loam. Further details of the paddy chronosequence can be found in Cheng et al. (2009) and Kölbl et al. (2014).

Sampling

The samples of soil cores from the chronosequence were obtained from a sampling campaign in June 2008 and collected in triplicate from three adjacent independent paddy fields, as described in e.g., Kalbitz et al. (2013) and Wissing et al. (2011). Paddy soil profiles with ages of 100 and 700 years, together with non-paddy fields with respective ages, hereafter named as SP-P100, SP-P700, SP-NP100, and SP-NP700, respectively, were used in the present study to investigate the variation of Fe concentration and isotope composition in the soil profiles between paddy and non-paddy fields. As this sampling campaign was performed after rice had been harvested, we carried out an additional sampling of the water-logged paddy topsoil and corresponding rice plants in September 2018 from the same chronosequence, when rice was in the transition from flowering to ripening stage. Also in triplicates, paddy fields with ages of 5, 50, 100, 300, 700, 1000, and 2000 years were sampled, hereafter named as P5, P50, etc. A non-paddy soil close to the paddy field of P700 was also collected in 2018, hereafter named NP. In addition, a tidal wetland soil was sampled on the sea side of the newly constructed dyke close to P5 (denoted as P0). At each sampling location, a soil core (0–20 cm) was taken from the submerged topsoil and sealed in a plastic zipper bag. Extra water that was present on top of the soil core was drained, while water within the soil core remained with the soil. As the water level in each field was different, the depth of the soil core finally collected varied between 12 to 22 cm. A hand-full of rice plants close to each soil sampling location, comprising 15 to 30 individual plants, was pulled out of the soil. The soil around the rice roots remained untouched until being processed in the labs of Ningbo

Observation and Research Station, Institute of Urban Environment (NUEORS), Chinese Academy of Sciences (CAS), China. The plants were wrapped in large plastic bags with roots being inserted into a plastic bag with a zipper lock. The plants were stored at 4 °C before they were cleaned by deionized water and separated into organs the day after the sampling. About half of the rice roots were immediately used to extract the Fe plaques as described below. The other half of the roots and other organs were frozen at –20 °C, freeze-dried before shipping to the Agrosphere Institute (IBG-3) at Forschungszentrum Jülich GmbH (FZJ), Germany.

Sample preparation

Digestion and extractions of soil

The soil of the soil profiles collected in 2008 were air-dried and was sieved to a size of <2 mm for a microwave-assisted digestion as described below. The other soils taken jointly with the rice plants in 2018 were freeze-dried in the NUEORS and shipped to the IBG-3, FZJ, Germany, for Fe concentration and isotope composition studies. At the IBG-3, the soil samples were milled to fine powders in a custom-designed ball mill (Collomix Viba 330, Collomix GmbH, Germany) using metal-free plastic bottles and tungsten carbide milling balls. About 0.05 g soil was added with a mixture of 3 ml distilled ultrapure HNO₃ (68%) and 1 ml H₂O₂ (30%, p.a.) in a pressurized microwave-assisted digestion system (turboWAVE, Milestone Srl, Italy). After a step-wised digestion program, the digested sample solutions were centrifuged at 5000×g for 10 min. While the undigested sand particles were discarded, the supernatant (Fe_{bulk}) was transferred into a round-bottomed 15-ml PFA vial (Savillex, Eden Prairie, USA) and placed on a heating plate at 80 °C to be completely dried down. The dried materials were re-dissolved in 1 ml 6 M HCl for further use. It is noteworthy that our digestion methods did not dissolve the Fe that had been sequestered in the silicates. As Kölbl et al. (2014) did not find significant differences in the assemblage of silicates in this chronosequence, it is therefore reasonable to assume that the variation of this Fe pool (i.e., silicate Fe) did not play a significant role in changes of the Fe_{bulk} as well as in rice nutrition in one growing season upon sampling.

To investigate Fe pools in soil, a sequential extraction of the topsoil was performed for 1) exchangeable and organically sorbed or bound Fe (Fe_{exch.+org.}) by a mixture of 0.01 M ultrapure HNO₃ and H₂O₂ (30%, p.a.), 2) short-range-ordered Fe oxides (Fe_{SRO}) by 0.5 M ultrapure HCl, and 3) crystalline Fe oxides (Fe_{cry.oxides}) by the conventional dithionite-citrate–bicarbonate (DCB) extraction. The amount of free Fe oxides was calculated as the sum of Fe_{SRO} and Fe_{cry.oxides}. The Fe pools by the sequential extractions were only analyzed for Fe concentration, but not for Fe isotope composition.

To estimate the plant-available Fe in soil samples (Fe_{HCl}, Guelke et al. 2010), 1 g soil was weighed into a Falcon® centrifuge tube and added with 20 ml 0.5 M ultrapure HCl. The soil-HCl mixture was shaken for 24 h using a rotator overhead shaker (BioSan Multi Bio RS-24, Germany) at room temperature and centrifuged at 5 000×g for 15 min. The residue was washed twice with Milli-Q water and the wash solution was combined with the extracted supernatant after centrifugation. The extract was then filtered through a PTFE filter with a pore-size of 0.45 µm and transferred into a round-bottomed 22-ml Savillex PFA vial. After drying down at 80 °C, 1 ml ultrapure HNO₃ (68%) was added to the sample before carefully adding 0.5 ml H₂O₂ (30%, p.a.). The vials were firmly closed and heated at 100 °C for 2 h to fully oxidize organic matters. The solution was then dried down again at 80 °C and re-dissolved in 1 ml 6 M ultrapure HCl for Fe purification.

Extraction of Fe plaques

The cleaned rice roots were merged in 200 ml 0.5 M HCl (p.a.) in an acid pre-cleaned glass beaker and placed in an ultrasonic bath for 15 min. After another two extractions by HCl, the roots were then rinsed twice in Milli-Q water for 15 min in the ultrasonic bath. The HCl-extract and the washed water were combined and heated at 90 °C to dryness and re-dissolved in 10 ml 6 M HCl. The concentrated extracts were sealed in metal-free plastic tubes and shipped to Germany. After the extraction, the roots looked pale in color, and the brownish color of the Fe plaques was slightly visible only at the basal root zone, indicating that majority of the Fe plaques was successfully removed from the root surface. The roots after

extraction were frozen at $-20\text{ }^{\circ}\text{C}$ and freeze-dried before shipping to Germany.

The concentrated extracts were transferred to a round-bottomed 22-ml Savillex PFA vial after being filtered through $0.45\text{ }\mu\text{m}$ PTFE filters. The original tube was washed by 3 ml 6 M ultrapure HCl for three times and the wash solution was combined with the extracts. The solution was then heated until dryness at $80\text{ }^{\circ}\text{C}$. After drying down, 1 ml ultrapure HNO_3 (68%) was added to the sample before carefully adding 0.5 ml H_2O_2 (30%, p.a.). The vials were firmly closed and heated at $100\text{ }^{\circ}\text{C}$ for 2 h to fully oxidize any organic matters. The solution was then dried down again at $80\text{ }^{\circ}\text{C}$ and re-dissolved in 1 ml 6 M ultrapure HCl for Fe purification.

Digestion of rice organs

The roots after the extraction of the Fe plaques, and the aboveground organs were weighted and then milled to fine powder in the ball mill. Fifty (roots) to two-hundred milligrams (aboveground) plant organs were weighted into a PFA (roots) or glass (aboveground) microwave extraction tube and mixed with 5 ml distilled ultrapure HNO_3 (68%) and 2 ml H_2O_2 (30%, p.a.) for the microwave-assisted digestion. The microwave-assisted digestion could not fully digest the plant samples, since the silicates that had been accumulated in the rice were preserved. Each individual extract was centrifuged at $5000\times g$ for 10 min and the supernatant was dried down in a round-bottomed 22-ml Savillex PFA vial at $80\text{ }^{\circ}\text{C}$. The dried materials were re-dissolved in 1 ml 6 M ultrapure HCl.

For all soil and plant samples, the concentrations of Fe and other nutrient elements (such as Mg, K, Ca, P, Mn, Cu, Zn, etc.) were analyzed by inductively coupled plasma mass spectrometry (ICP-MS, Agilent 7900, Agilent, Germany) with uncertainty of max. 5%. An in-house standard for soil (Luvisol, collected at Klein-Altendorf Experimental Station ($50^{\circ}37'9''\text{N}$, $6^{\circ}59'29''\text{E}$) of the University of Bonn, Germany, Fe concentration $20.1\pm 0.6\text{ g kg}^{-1}$, $\delta^{56}\text{Fe} = -0.01\pm 0.03\text{‰}$, $n=18$) and NIST SRM 1575a (Fe concentration $43.5\pm 0.8\text{ g kg}^{-1}$, $\delta^{56}\text{Fe} = -1.52\pm 0.08\text{‰}$, $n=13$) were processed for digestion as routine standards for soil and plant, respectively, in parallel with the samples in each analytical batch to validate the experimental and analytical procedures.

Iron purification and isotope analysis

The dry-down processes and Fe purification were performed in customer-designed laminar flow box in a cleanroom at IBG-3, FZJ. Iron purification was carried out using anion exchange chromatography resin (Bio-Rad AG1-X4, 200–400 mesh, Dauphas et al. 2004). Aliquots of the 6 M HCl-re-dissolved samples containing $10\text{ }\mu\text{g}$ Fe were loaded on 1 ml resin. The matrix elements were stepwise eluted by in total 10 ml 6 M ultrapure HCl (matrix cut) and then Fe was stepwise eluted by in total 6 ml 0.05 M ultrapure HCl (for soil) or by 1.5 M ultrapure HCl (for plants due to relatively larger Zn: Fe ratios) (Fe cut). The Fe cut was then dried down at $80\text{ }^{\circ}\text{C}$ and re-dissolved in 1 ml 0.3 M ultrapure HNO_3 for Fe isotope analysis. Good recovery of Fe ($>95\%$) and the absence of matrix elements were confirmed by analyzing Fe and other elements (e.g., Al, Si, Mg, Ca, K, Mn, Cu, Zn, etc.) in the Fe cut by ICP-MS. A dissolved sample of Fe isotope standard IRMM-524a and an acid blank were processed in parallel with the samples in each batch of column chromatography for quality control.

Iron isotope analysis was performed on multi-collector ICP-MS (MC-ICP-MS, Nu Plasma II, Nu Instruments Ltd., UK) coupled with a desolvating nebulizer system (Aridus II, Teledyne Cetac, USA), in high mass resolution mode with a mass resolving power ($\text{Rp}_{5,95\%}$) of >8000 at ion beam transmission of 10%. To correct instrumental mass bias, a strategy of standard-sample-standard bracketing was applied using IRMM-524a as the standard with a matched Fe concentration (500 ppb) and a matched acid molarity (0.3 M HNO_3) to the samples. The results of Fe isotope analysis in samples were expressed using IRMM-014 as the standard (Dauphas et al. 2017), as IRMM-524a is the original material of IRMM-014:

$$\delta^{56}\text{Fe}(\text{‰}) = \left(\frac{\frac{{}^{56}\text{Fe}_{\text{sample}}}{{}^{54}\text{Fe}_{\text{sample}}}}{\frac{{}^{56}\text{Fe}_{\text{IRMM-014}}}{{}^{54}\text{Fe}_{\text{IRMM-014}}}} - 1 \right) * 1000$$

Both $\delta^{56}\text{Fe}$ and $\delta^{57}\text{Fe}$ were analyzed to evaluate any possible mass-independent isotope fractionation during the analysis. In addition, signals of ^{53}Cr were monitored in order to correct any possible interference of ^{54}Cr on ^{54}Fe . Long-term external precision was achieved at 0.08‰ and 0.12‰ for $\delta^{56}\text{Fe}$ and

$\delta^{57}\text{Fe}$, respectively, based on two times the standard deviation (SD) of the $\delta^{56}\text{Fe}$ and $\delta^{57}\text{Fe}$ values of the repeated measurement of the IRMM-524a during the analytical sessions.

Data calculation, error propagation and statistics

The Fe concentration and isotope composition of soil and plant were given as the mean value of the three field replicates and the standard error (SE) of the mean, unless it was specifically stated.

The Fe isotope compositions of aboveground shoot ($\delta^{56}\text{Fe}_{\text{shoot}}$) and of the whole plant ($\delta^{56}\text{Fe}_{\text{whole plant}}$) were calculated based on mass balance using:

$$\delta^{56}\text{Fe}_{\text{shoot/wholeplant}} = \sum \left(\delta^{56}\text{Fe}_i \times \frac{m_i c_i}{\sum m_i c_i} \right)$$

where m_i and c_i were the dry biomass and the Fe concentration of plant organ i (root, stem, leaf, or ear), respectively.

The 2SD of the calculated Fe isotope composition of the aboveground shoot or the whole plant of individual field replicate was computed as follows:

$$2SD_{\text{shoot/wholeplant}} = \sqrt{\sum \left(2SD_i \times \frac{m_i c_i}{\sum m_i c_i} \right)^2}$$

where m_i and c_i were the dry biomass and the Fe concentration of plant organ i (root, stem, leaf, or ear), respectively.

The apparent difference in Fe isotope composition in two Fe pools, A and B, such as Fe in the whole rice plant, Fe in the shoot, Fe in the Fe plaques, the plant-available Fe, etc., were calculated using:

$$\Delta^{56}\text{Fe}_{A-B} = \delta^{56}\text{Fe}_A - \delta^{56}\text{Fe}_B$$

The 2SD of the apparent difference of Fe isotope compositions between two Fe pools A and B of individual field replicates was computed as follows:

$$2SD_{\Delta^{56}\text{Fe}_{A-B}} = \sqrt{(2SD_{\delta^{56}\text{Fe}_A})^2 + (2SD_{\delta^{56}\text{Fe}_B})^2}$$

Statistical analyses and mathematic fittings were performed using OriginPro (Version 2019; OriginLab 2019). The significance of differences in Fe concentration and isotope composition between samples from fields with two different ages of rice cultivation was assessed by performing two-sample t-test

following an F-test for testing equality of variances. Significance of differences was accepted at $p < 0.05$. If a significant difference accrued, we performed the least-significant-difference procedure.

Results

Iron concentration and isotope composition of the soil

The paddy soil profiles showed larger variation of the Fe concentration through the profiles than their non-paddy counterparts (Fig. SII). In these drained soil profiles, we did not observe a difference in Fe concentrations in the surface soil (0–10 cm) between paddy and non-paddy fields. However, a smaller Fe concentration was found below the surface layer (10–50 cm) in P700, suggesting that prolonged paddy land-use promoted an Fe leaching from these horizons to deeper ones (50–100 cm), which thus showed larger Fe concentration than the non-paddy fields. Large heterogeneity regarding Fe concentration was observed among paddy field replicates, especially in deeper horizons, which we attribute to the illuviation and zonation of Fe in the subsoil. We thus did not continue to investigate changes in Fe pools across different soil horizons. Nevertheless, it seems that the decreased Fe concentration in soil horizons above 50 cm went along with a heavier Fe isotope composition compared with the non-paddy fields, and the increased Fe concentration in soil horizons 50–75 cm was accompanied with a lighter Fe isotope composition, although the differences were not significant due to large heterogeneity. Therefore, similar to Fe concentration, the variation of the $\delta^{56}\text{Fe}$ values through the profile was larger in the paddy fields ($\Delta^{56}\text{Fe}_{\text{profile-paddy}} = 0.08\text{‰}$ vs. $\Delta^{56}\text{Fe}_{\text{profile-non-paddy}} = 0.03\text{‰}$, Fig. SII).

In the water-logged topsoil (on average 0–20 cm), we found a linear decreasing trend in Fe concentration with increasing rice cultivation age (Fig. 1, Table SII). The Fe concentration in the field P2000 was the smallest ($\text{Fe}_{\text{P2000}} = 20.8 \pm 0.4 \text{ g kg}^{-1}$) and only two-third of that of the parent material (tidal wetland, $\text{Fe}_{\text{P0}} = 30.1 \pm 0.9 \text{ g kg}^{-1}$). Regression fitting suggested that, on average, each year of paddy management resulted in a loss of 5 mg Fe kg^{-1} soil (5 g kg^{-1} in 1000 years; Fig. 1). Using an average bulk density

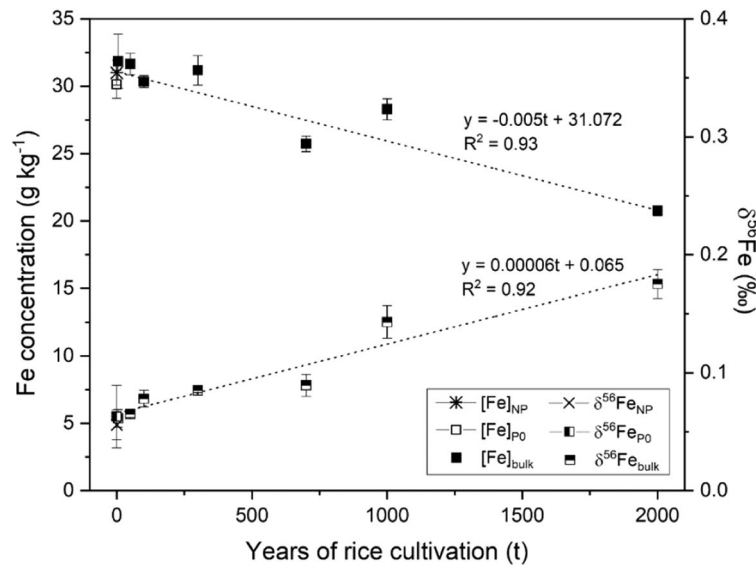


Fig. 1 Total Fe concentration ([Fe]) and isotope composition ($\delta^{56}\text{Fe}$) of the topsoil of the paddy chronosequence (Fe_{bulk} , rice cultivation time of 5, 50, 100, 300, 700, 1000, and 2000 years, respectively), of the topsoil of a non-paddy soil (Fe_{NP} , adjacent to P700), and of a tidal wetland soil (Fe_{P0} , adjacent to P5). Error bars represent the standard error of the mean of three

filed replicates. The dotted lines are linear fittings of the Fe concentration and the $\delta^{56}\text{Fe}_{\text{bulk}}$ values to the years of rice cultivation (t), respectively, with fitting equations and R^2 above the respective fitting line. Mathematic fitting results can be found in Table SII

of 1.2 kg dm^{-3} for the top 20 cm of soil (Kölbl et al. 2014), this corresponds to an average Fe loss rate of $12 \text{ kg Fe ha}^{-1} \text{ yr}^{-1}$, and $24\,000 \text{ kg Fe ha}^{-1}$ in total after 2000 years of paddy land-use (corresponding to 33% of total Fe of the parent material).

Along with this Fe loss, the Fe isotope composition of the topsoil became increasingly heavier (Fig. 1). The $\delta^{56}\text{Fe}_{\text{P2000}}$ value was $0.11 \pm 0.03\text{‰}$ isotopically heavier than that of the parent material ($\delta^{56}\text{Fe}_{\text{P0}} = 0.06 \pm 0.03\text{‰}$). A linear fitting of the $\delta^{56}\text{Fe}$ values suggested an Fe isotope fractionation of about 0.06‰ per 1000 years of paddy management for an Fe loss rate of $12 \text{ kg Fe ha}^{-1} \text{ yr}^{-1}$. In other words, at our study site with a parent material containing $30.1 \text{ g kg}^{-1} \text{ Fe}$, to reach an Fe isotope fractionation of 0.01‰ , the soils must lose $2 \text{ kg}^{-1} \text{ Fe ha}^{-1}$ or 2.7% of its Fe as a result of a redox oscillation and leaching. By contrast, long-term managed non-paddy soil had retained the Fe concentration and isotope composition of the parent material (Fig. 1). In this sense, our data support our first hypothesis that it seems possible to scale the duration of anthropogenic paddy land-use by Fe loss and related Fe isotope fractionation, or,

vice versa, to use changes of the latter relative to the parent material to reconstruct paddy land-use ages.

Figure 2 shows that the loss of Fe_{bulk} along the rice cultivation coincided with a loss of Fe minerals, including short-range-ordered (Fe_{SRO}) and crystalline Fe oxides ($\text{Fe}_{\text{cry.oxides}}$). However, unlike bulk Fe, the losses of the Fe oxide fractions were not linear but followed exponential declines (Table SII). Noticeably, it seems that $\text{Fe}_{\text{cry.oxides}}$ still proceeded with the decline after 2000 years of paddy management, while the decrease of Fe_{SRO} levelled out after a millennium. In contrast to Fe oxides, the concentration of $\text{Fe}_{\text{exch.+org.}}$ increased significantly soon after paddy land-use, and continuously became larger following an exponential growth trend. By the time of sampling, the intensively managed paddy fields P2000 contained almost 200-fold of the $\text{Fe}_{\text{exch.+org.}}$ concentrations in P5 ($1.805 \pm 0.042 \text{ g kg}^{-1}$ vs. $0.009 \pm 0.001 \text{ g kg}^{-1}$). However, the extent to which $\text{Fe}_{\text{exch.+org.}}$ concentrations increased did not match the loss of Fe_{SRO} and $\text{Fe}_{\text{cry.oxides}}$ along the paddy chronosequence, as the total amount of Fe extracted by the sequential extraction decreased in half from

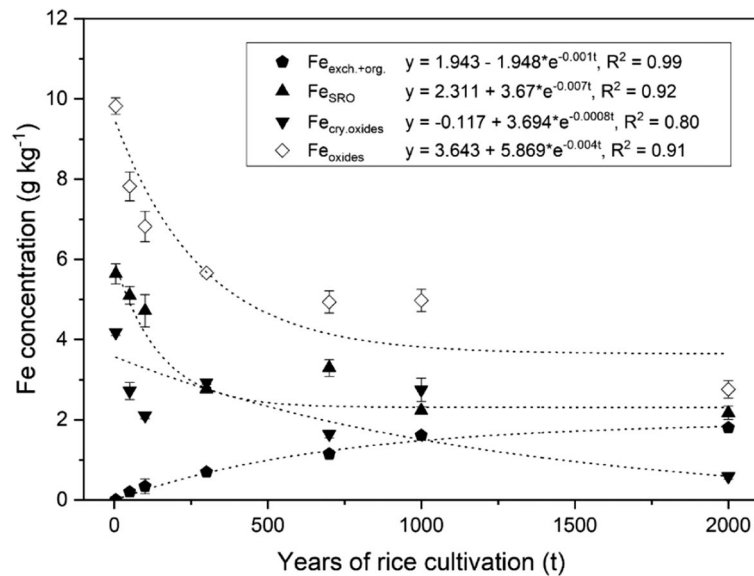


Fig. 2 Iron concentration of exchangeable and organically sorbed or bound ($\text{Fe}_{\text{exch.}+\text{org.}}$), short-range-ordered Fe minerals (Fe_{SRO}), crystalline Fe oxides ($\text{Fe}_{\text{cry.oxides}}$), which were extracted sequentially, and free Fe oxides as the sum of Fe_{SRO} and $\text{Fe}_{\text{cry.oxides}}$ ($\text{Fe}_{\text{oxides}}$). Error bars represent the standard error

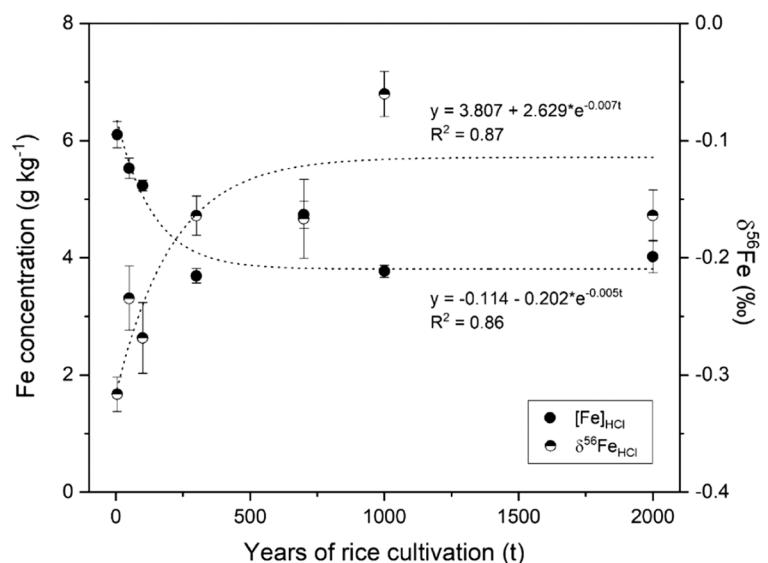
of the mean of three filed replicates. The dotted lines are exponential fittings of the concentrations of Fe_{SRO} , $\text{Fe}_{\text{cry.oxides}}$ and $\text{Fe}_{\text{oxides}}$ to the years of rice cultivation (t), respectively, with fitting equations and R^2 following respective legend. Mathematic fitting results can be found in Table SII

$9.8 \pm 0.2 \text{ g kg}^{-1}$ to $4.6 \pm 0.2 \text{ g kg}^{-1}$, which overall led to a loss of total Fe.

The $\text{Fe}_{\text{exch.}+\text{org.}}$ and Fe_{SRO} pools are considered to be available to plants. They together can be extracted by diluted HCl that can be further used for the determination of its Fe isotope composition

without risking isotope fractionation during the extraction (Wiederhold et al. 2007). Clearly, the plant-available pool (Fe_{HCl}) also followed an exponential decline along the paddy ages with a decay constant close to that of Fe_{SRO} (Fig. 3). Because of this exponential decline, Fe_{HCl} had already lost one

Fig. 3 Iron concentration and isotope composition of HCl-extractable Fe in the paddy chronosequence. Error bars represent the standard error of the mean of three filed replicates. The dotted lines are exponential fittings of the Fe concentrations and the $\delta^{56}\text{Fe}_{\text{HCl}}$ values to the years of rice cultivation (t), respectively, with fitting equations and R^2 close to the respective fitting line. Mathematic fitting results can be found in Table SII



third of the total Fe_{HCl} in the first hundreds of years after reclamation (≤ 300 years). Concomitantly, the $\delta^{56}\text{Fe}_{\text{HCl}}$ values increased by 0.15‰ . Along with the continuous rice cultivation, both concentration and isotope composition of Fe_{HCl} tended to reach a steady state at about 3.8 g kg^{-1} and -0.11‰ , respectively. This is opposite to the changes in Fe_{bulk} , which continued to be lost after prolonged paddy land-use (> 300 years). Obviously, there was some neo-formation of plant-available Fe_{HCl} despite ongoing Fe loss. In addition, the $\delta^{56}\text{Fe}_{\text{HCl}}$ values were correlated with Fe_{HCl} concentration (Fig. SI2, Pearson's $r = -0.91$), indicating that the overall loss of $1 \text{ g Fe}_{\text{HCl}}$ from 1 kg soil would result in the $\delta^{56}\text{Fe}_{\text{HCl}}$ value to increase by about 0.08‰ , and

this process was accomplished in the first hundreds years.

Iron concentration and isotope composition of rice plant

The Fe concentration of rice roots increased along with the paddy ages ($R^2 = 0.73$) and were considerably larger than those of aboveground organs, which showed a similar concentration in different paddy fields (Fig. 4a). As a result, the Fe concentration in the whole plants increased with increasing duration of paddy management (Fig. 4b, $R^2 = 0.90$). In addition, both mean biomass and mean Fe content per rice plant increased linearly along the paddy ages

Fig. 4 Iron concentration of the rice organs (a) and of the aboveground shoot and the whole plant (b). Error bars represent the standard error of the mean of three filed replicates. The black dotted lines are linear fittings of the Fe concentrations of the root and the whole rice plant to the years of rice cultivation (t), respectively, with fitting equations and R^2 close to the respective fitting line. Mathematic fitting results can be found in Table SI1. The grayish solid lines are present to ease the identification of data of the same organs along the years of rice cultivation, for which no consistent trends were found

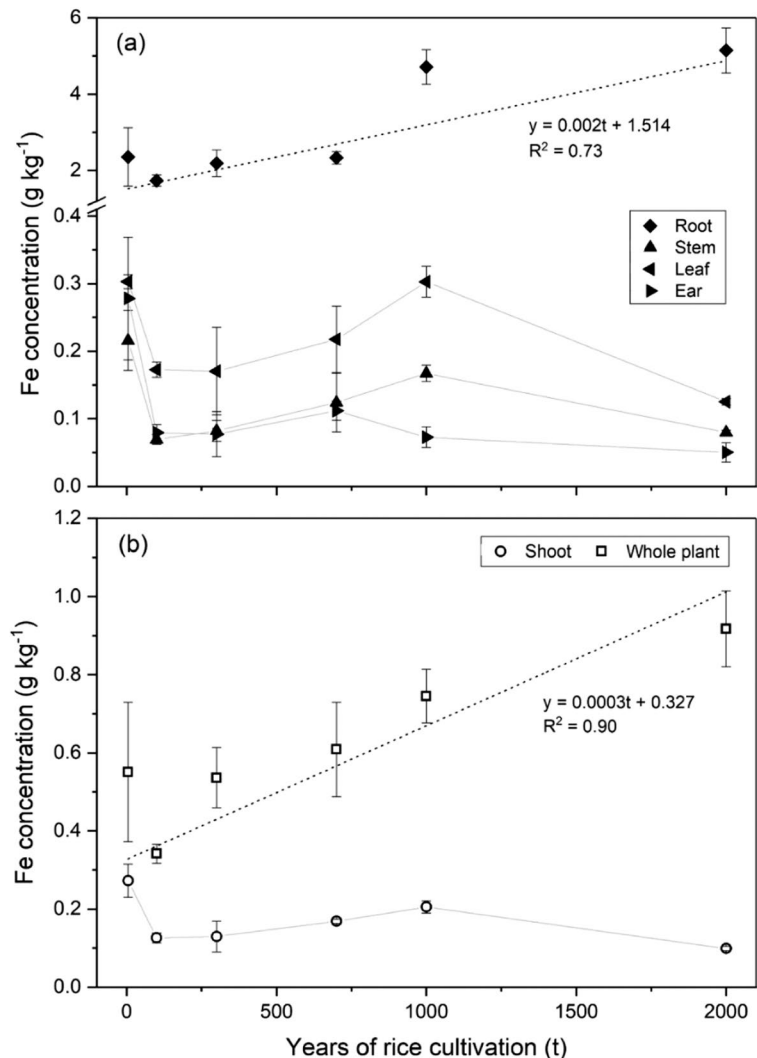


(Fig. S14). In this regard, Fe concentrations in the rice plant behaved almost oppositely to those in the plant-available Fe_{HCl} pool (Fig. 3).

The Fe isotope composition of rice roots ($\delta^{56}\text{Fe}_{\text{root}}$) ranged between $0.04 \pm 0.00\text{‰}$ to $0.22 \pm 0.02\text{‰}$ (the mean and its standard error (SE, same below) of three field replicates, Fig. 5a), similar or slightly heavier than the $\delta^{56}\text{Fe}_{\text{bulk}}$ values (Fig. 1), but significantly heavier than the $\delta^{56}\text{Fe}_{\text{HCl}}$ values (Fig. 3) in respective paddy fields. The aboveground organs were all enriched in light Fe isotopes, with the $\delta^{56}\text{Fe}$ values ranging from $-0.45 \pm 0.03\text{‰}$ to $-0.07 \pm 0.01\text{‰}$ (the mean and its SE of three field replicates). These values, except for those of leaves, showed little, if any, consistent trends along the ages of paddy

management. The Fe isotope composition of the whole rice plants seemed to follow an exponential trend, which increased rapidly after paddy land-use and then remained similar within uncertainty, with an average $\delta^{56}\text{Fe}$ value of $0.01 \pm 0.07\text{‰}$ cross all fields (Fig. 5b). On the other hand, we did not find any consistent trend for the $\delta^{56}\text{Fe}$ values of the shoots.

The $\delta^{56}\text{Fe}_{\text{plaque}}$ values were all heavier than all the soil and plant samples, ranging from $0.08 \pm 0.03\text{‰}$ to $0.66 \pm 0.03\text{‰}$ (the mean and its SE of three field replicates, Fig. 6). Even though we did not find any trend for the $\delta^{56}\text{Fe}_{\text{plaque}}$ values along the age of paddy fields, we observed a close relation between the $\delta^{56}\text{Fe}_{\text{plaque}}$ and the $\delta^{56}\text{Fe}_{\text{whole plant}}$ or the $\delta^{56}\text{Fe}_{\text{root}}$ values (Pearson's $r=0.97$, and 0.66 , respectively). Yet, similar

Fig. 5 Iron isotope composition of the rice organs (a) and of the aboveground shoot and the whole plant (b). Error bars represent the standard error of the mean of three filed replicates. The black dotted lines are exponential fittings of the $\delta^{56}\text{Fe}$ values of the leaf and the whole rice plant to the years of rice cultivation (t), respectively, with fitting equations and R^2 close to the respective fitting line. Mathematic fitting results can be found in Table S11. The grayish solid lines are present to ease the identification of data of the same organs along the years of rice cultivation, for which no consistent trends were found

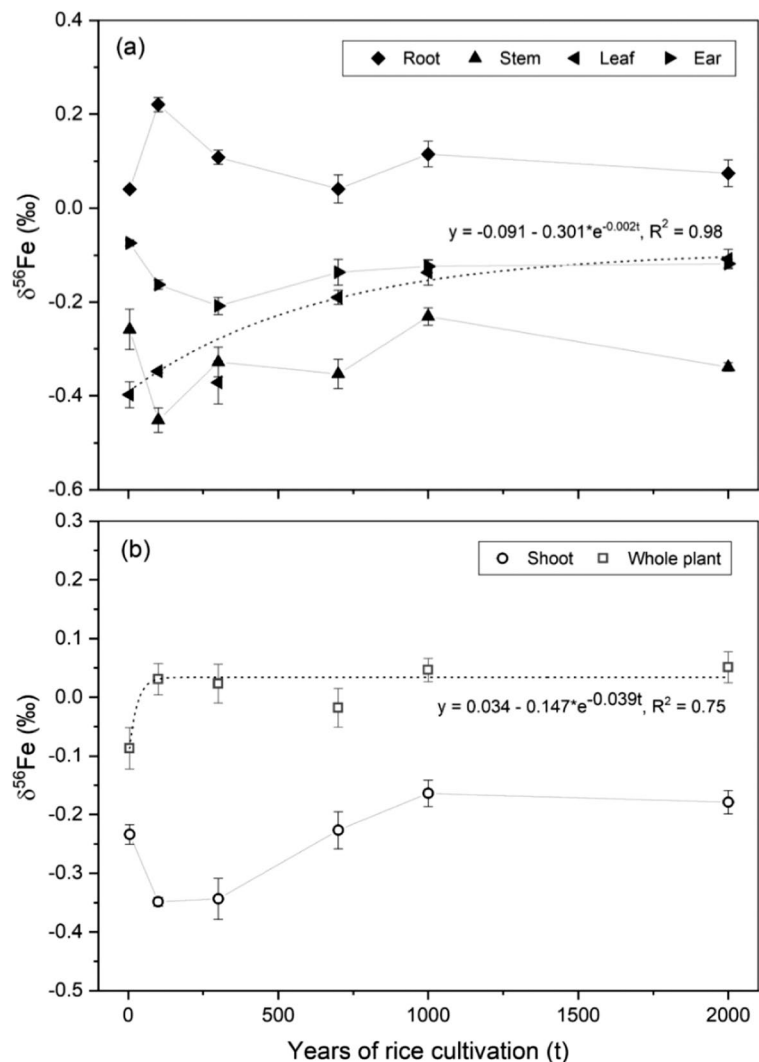
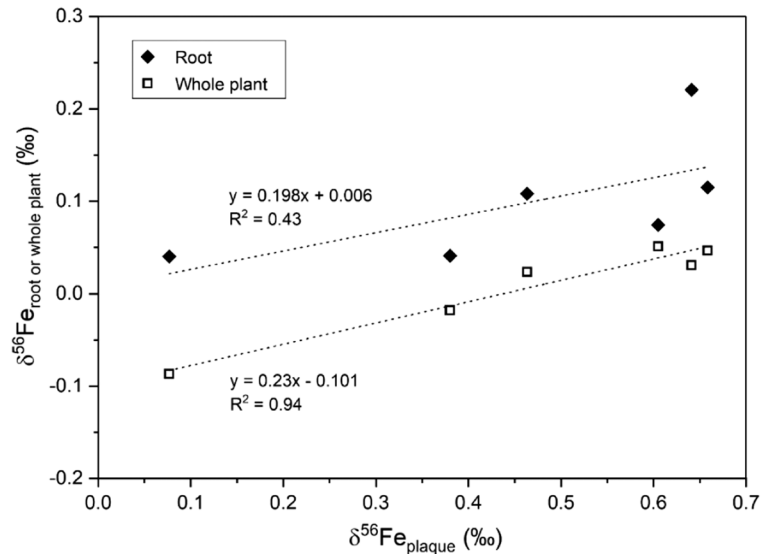


Fig. 6 Iron isotope composition of the rice root and the whole plant in relation with that of the Fe plaques. The dotted lines are the linear fittings of the $\delta^{56}\text{Fe}_{\text{root}}$ and the $\delta^{56}\text{Fe}_{\text{whole plant}}$ values to corresponding $\delta^{56}\text{Fe}_{\text{plaque}}$ values with Pearson's $r=0.66$ and 0.97 , respectively, with fitting equations and R^2 close to the respective fitting line. Mathematic fitting results can be found in Table S11



relation was not observed between the $\delta^{56}\text{Fe}_{\text{whole plant}}$ or the $\delta^{56}\text{Fe}_{\text{root}}$ and the $\delta^{56}\text{Fe}_{\text{HCl}}$ values (Fig. S13), suggesting that the Fe plaques, rather than the plant-available Fe pool in soil, might have directly contributed to the uptake of Fe in rice. In this sense, testing our second aim showed that the Fe isotope composition of rice plants resembles that of Fe plaques but not that of soil, irrespective to the duration of paddy soil management.

Discussion

Iron dynamics in the paddy chronosequence

In paddy soils, Fe cycling is controlled by the redox potential variation, which plays an important role in the functioning of the system. Iron transformation and translocation, as well as the accrual of soil organic matter (SOM; Kalbitz et al. 2013; Kögel-Knabner et al. 2010; Kölbl et al. 2014), as a result of paddy management, lead to characteristic paddy profiles. When flooded, structural Fe in clay minerals is released by microbial utilization of DOM as electron donors (e.g., Li et al. 2004), and then transformed to ferrihydrites via aqueous organic Fe(III) complexes (Suetsugu et al. 2005). Repeated redox cycles promote a redistribution of Fe oxides in soil profiles (Wissing et al. 2013, 2014; Zhang and Gong 2003) and crystallinity (Kölbl et al. 2014; Thompson et al. 2006).

With prolonged ages of paddy soil management, dissolution and subsequent eluviation of Fe upon reduction is enhanced with downward leaching and successive re-precipitation, forming an Fe-enriched illuvial horizon at depth, as shown in the Fe concentration profiles of the two paddy fields (Fig. S11). The illuvial horizon exhibits a lighter Fe isotope composition than the eluvial horizon (Fig. S11; see also Huang et al. 2018). The topsoil, however, may progressively lose Fe if the Fe influx through irrigation or return of rice straws cannot compensate Fe leaching and lateral drainage. Indeed, in our paddy chronosequence, Fe concentration in topsoil decreased along the paddy ages. After 2000 years of paddy land-use, Fe concentration in topsoil was only two-third of that in its parent material (Fig. 1).

The loss of Fe concentration from topsoil affected Fe oxides with all crystallinities, thus reflecting that redox potential were low enough to dissolve all Fe oxides. This is contrast to previous findings by Cheng et al. (2009) and Wissing et al. (2013), where no systematic trend for free Fe oxides in the chronosequence was found. Also, Huang et al. (2018) revealed a decrease in oxide bound Fe, but the extent and rate of the decline was not as extensive as our results. We attribute these differences to the time of sampling: in these cited studies the soil was sampled while drained, while here we sampled the soil under submerged conditions. Hence, there was also likely a seasonal dynamics of Fe, with parts of the Fe lost being

replaced by residue return or capillary rise during the dry periods.

As paddy management prolonged (> 300 years), the decline in Fe had already occurred to an extent that Fe isotope composition of the bulk topsoil became progressively heavier as a collective result of preferential dissolution and subsequent removal of light Fe isotopes as Fe^{2+} and organic Fe(III) complexes. In addition, while the $\text{Fe}_{\text{cry.oxides}}$ continuously declined, the Fe_{SRO} reached a rather steady-state (Fig. 2), thus supporting the idea of a profound consumption and transformation from crystalline Fe oxides to those with less crystallinity under anaerobic conditions. On the other hand, the rate of crystallization of Fe oxides from the newly formed Fe_{SRO} was insufficiently fast, so that $\text{Fe}_{\text{cry.oxides}}$ was further depleted in older paddy fields. This observation contradicts previous findings that the crystallinity of Fe oxides increases upon redox oscillations on short-time scale as shown by Thompson et al. (2006). We attribute this difference to the fact that the two investigated systems are distinct in three main aspects: 1) our paddy fields experienced considerably longer redox oscillations (millennium vs. days), 2) the studied paddy topsoils are open systems where continuous Fe exchanges between environmental compartments due to e.g., leaching, uptake by rice plants take place, and 3) the life cycles of rice plants and the contribution of organically associated Fe to the Fe dynamic are absent in Thompson et al. (2006). We conclude that Fe dynamics under long-term field conditions likely differ from those in short-term soil incubation experiments, and that the effects of plants on soil Fe cycles cannot be neglected. Repeated residue return likely contributed to the rise of $\text{Fe}_{\text{exch.+org.}}$ pool, either because they contained Fe, or because they additionally served as bonding partner similar to inherent SOM for dissolved Fe. Similarly, increased concentrations of dissolved organic carbon (Kölbl et al. 2014) co-precipitated with Fe(III), mostly with Fe_{SRO} such as ferrihydrites (Suetsugu et al. 2005), thus additionally promoting the accumulation of organically bound/sorbed Fe.

Plant-available Fe and the Fe source of rice

Plant-available Fe pool consists of water-soluble, exchangeable, organically bound/sorbed Fe and Fe_{SRO} (Fe_{HCl} , Guelke et al. 2010; Wiederhold et al. 2007). In

our study, Fe_{HCl} thus equals to the sum of $\text{Fe}_{\text{exch.+org.}}$ and Fe_{SRO} . Indeed, $\text{Fe}_{\text{exch.+org.}}$ and Fe_{SRO} recovered almost the entire Fe_{HCl} pool ($96 \pm 3\%$), the remaining difference reflecting operational and analytical errors. Within the Fe_{HCl} pool, the contribution of $\text{Fe}_{\text{exch.+org.}}$ became increasingly important, as Fe that had been taken up by crops was intensively recycled in the topsoil and residue return provided a growing number of bonding positions for the dissolved Fe.

The linear relation between the decreased Fe_{HCl} concentration and the increased $\delta^{56}\text{Fe}_{\text{HCl}}$ values (Fig. 3) reflects an observable response of Fe isotope composition to the changes of not only the pool size, but also of Fe species in this pool, which were accompanied by losses of light Fe with repeated flooding, harvesting and leaching. As these losses of Fe always occur, Fe_{HCl} must have been replenished to reach steady state as observed. This replenishment should also have happened when Fe_{HCl} was still depleting from the topsoil, as neo-formation of Fe_{SRO} took place whenever water was drained and accumulation of $\text{Fe}_{\text{exch.+org.}}$ occurred along the paddy land-use. In this sense, their formation and accumulation with a relatively heavier $\delta^{56}\text{Fe}$ values also contributed to the trend that the $\delta^{56}\text{Fe}_{\text{HCl}}$ values became heavier. In other words, the majority of the pristine Fe_{HCl} pool was likely gradually replaced by isotopically heavier newly-formed Fe_{SRO} and $\text{Fe}_{\text{exch.+org.}}$ before reaching the steady state. Afterwards, the Fe_{HCl} pool was in equilibrium between depletion and replenishment, and the Fe leaving and entering the Fe_{HCl} pool was in a similar amount and exhibited similar Fe isotope composition.

The changes (losses) of the plant-available Fe did not impact the growth of the rice plants, as an increase in both mean biomass and Fe content was observed in rice plants with increased duration of paddy land-use (Fig. SI4) and the Fe isotope composition of rice was independent on that of the plant-available Fe (Fig. SI3). In the P5 field, mean biomass was the smallest and Fe concentration was the largest, presumably reflecting resistance to the high salinity shortly after reclamation. As a rapid desalinization took place in the first few decades (Chen et al. 2011), rice growth in older fields was improved rapidly, suggesting a higher Fe use efficiency with increases in paddy ages. However, the increased Fe content was mainly attributed to the rice roots, reflecting plants' homeostasis by Fe retention in the roots (Aung and Masuda 2020). As a result, the majority of Fe in rice retained in the paddy fields and recycled as a part of the plant-available Fe.

At our study sites, the Fe supply in soil was sufficient for plant growth. Without Fe deficiency, rice in these fields will likely not utilize strategy II to obtain Fe from soil, as they can directly acquire Fe(II) dissolved in the soil water (Kobayashi and Nishizawa 2012). This process should lead to a light isotopic Fe signature in plants, as paddy soil water was characterized by a very light Fe isotope composition (e.g., -0.80 to -3.40‰ in the study of Garnier et al. 2017). However, the $\delta^{56}\text{Fe}$ values of our rice plants were close to 0‰ (Fig. 5b), indicating that a different Fe pool served at least partially as the Fe source, and that this pool was not the isotopically light plant-available Fe pool in soil either, as the latter did not correlate with $\delta^{56}\text{Fe}_{\text{whole plant}}$ values (Fig. SI3). Yet, the rice roots were covered by a layer of the Fe plaques due to oxygen release by rice roots into the rhizosphere (Kirk et al. 1990). These Fe plaques exhibited as a barrier between the rice roots and the dissolved Fe(II) (Becker and Asch 2005), depending on how dense they were formed on the root surface. The Fe source of the plants may thus be supplemented by Fe from the plaques, as proposed by Garnier et al. (2017) and Chen et al. (2021). As the Fe plaques are Fe oxides, the chelation strategy via phytosiderophores (PS) is needed for rice to acquire Fe, leading to the rice plant displaying heavier Fe isotope composition compared with that if direct uptake from the aqueous Fe(II) took place (Wu et al. 2019). Here, the $\delta^{56}\text{Fe}$ values of the Fe plaques were heavier than those of rice but also in correlation with the latter, suggesting that the Fe plaques played a major role in the uptake, and during the uptake there was either an isotope fractionation induced by chelation and transformation from Fe oxides to Fe complex in the roots or a combination of chelation strategy and direct uptake of Fe^{2+} , or both. The latter may be a result of reduction of the Fe plaques by Fe-reducing microorganisms such as *Geobacter* that are abundant in the rhizosphere of rice (Wang and Liu 1992). However, we did not find a constant difference in isotope composition between respective $\delta^{56}\text{Fe}_{\text{root}}$ or $\delta^{56}\text{Fe}_{\text{whole plant}}$ and $\delta^{56}\text{Fe}_{\text{plaque}}$ values along the chronosequence, suggesting that the uptake-derived isotope fractionation may likely depend on local conditions that differ among the fields. These conditions can be, among others, Fe species in the Fe plaques, rice variety, and the structures and activities of the microorganism community in the rhizosphere that may impact the uptake.

Conclusion

Our present study showed that long-term paddy soil management resulted in significant variation of Fe isotope composition. The respective changes in the Fe isotope composition in soil occurred at a millennium scale, while internal changes and transformation among soil Fe pools took place already within decades of paddy use. As the duration of paddy management proceeded, Fe in topsoil was not only partly lost but also re-distributed from crystalline Fe oxide pools to organically sorbed/bound Fe, reflecting an enhanced coupling of the Fe nutrient cycle to that of soil organic carbon. The organically associated Fe complexes played an increasingly important role in releasing Fe(II) to soil solution, which was then re-precipitated as Fe plaques on the rice root surface, and finally acquired by the plants. Overall, our study demonstrated that anthropogenic activities such as long-term paddy management have impacted the terrestrial Fe cycle by altering the abiotic and biotic processes that have left a fingerprint in the ecosystem.

Acknowledgements We thank Dr. Ping Zou at Zhejiang Academy of Agricultural Sciences, Hangzhou, China, and Dr. Yaying Li at Ningbo Observation and Research Station, Institute of Urban Environment, Chinese Academy of Sciences, Ningbo, China, for the soil and plant sampling in September 2018. Prof. Dr. Roland Bol at Institute of Bio- and Geosciences: Agrosphere, Forschungszentrum Jülich GmbH, Germany, is acknowledged for proof reading of the manuscript as an internal reviewer. We appreciate the support of German Research Foundation (DFG) for this work with the project number 391749090.

Author contribution Bei Wu and Wulf Amelung developed the study conception and design. Huaiying Yao developed the design and organized the study at the Chinese sites. Wulf Amelung carried out sampling in 2008, while Bei Wu, Xiangtian Meng and Huaiying Yao performed sampling in 2018. Sample preparation was performed by Bei Wu and Xiangtian Meng. Data acquisition and analysis were performed by Bei Wu. The first draft of the manuscript was written by Bei Wu and all authors commented on previous versions of the manuscript. All authors read and approved the final manuscript.

Funding Open Access funding enabled and organized by Projekt DEAL. This work was supported by German Research Foundation (DFG) for funding the joint Sino-German research project “Iron dynamics in paddy soil chronosequence in view of stable iron isotope signature and iron speciation” (project number 391749090).

Data availability The dataset generated during the current study is provided as electronic supplementary material.

Declarations

Competing interests The authors declare that they have no conflict of interest.

Open Access This article is licensed under a Creative Commons Attribution 4.0 International License, which permits use, sharing, adaptation, distribution and reproduction in any medium or format, as long as you give appropriate credit to the original author(s) and the source, provide a link to the Creative Commons licence, and indicate if changes were made. The images or other third party material in this article are included in the article's Creative Commons licence, unless indicated otherwise in a credit line to the material. If material is not included in the article's Creative Commons licence and your intended use is not permitted by statutory regulation or exceeds the permitted use, you will need to obtain permission directly from the copyright holder. To view a copy of this licence, visit <http://creativecommons.org/licenses/by/4.0/>.

References

- Amaral DC, Lopes G, Guilherme LRG, Seyfferth AL (2017) A new approach to sampling intact Fe plaque reveals Si-induced changes in Fe mineral composition and shoot as in rice. *Environ Sci Technol* 51:38–45. <https://doi.org/10.1021/acs.est.6b03558>
- Aung MS, Masuda H (2020) How does rice defend against excess iron?: physiological and molecular mechanisms. *Front Plant Sci* 11:1102. <https://doi.org/10.3389/fpls.2020.01102>
- Becker M, Asch F (2005) Iron toxicity in rice - conditions and management concepts. *J Plant Nutr Soil Sci* 168:558–573. <https://doi.org/10.1002/jpln.200520504>
- Bughio N, Yamaguchi H, Nishizawa NK, Nakanishi H, Mori S (2002) Cloning an iron-regulated metal transporter from rice. *J Exp Bot* 53:1677–1682. <https://doi.org/10.1093/jxb/erf004>
- Chen LM, Zhang GL, Effland WR (2011) Soil characteristic response times and pedogenic thresholds during the 1000-year evolution of a paddy soil chronosequence. *Soil Sci Soc Am J* 75:1807–1820. <https://doi.org/10.2136/sssaj2011.0006>
- Chen G, Liu T, Li Y, Gao T, Huang F, Li X, Zhong S, Li F (2021) New insight into iron biogeochemical cycling in soil-rice plant system using iron isotope fractionation. *Fundam Res* 1:277–284. <https://doi.org/10.1016/j.fmr.2021.04.006>
- Cheng YQ, Yang LZ, Cao ZH, Yin S (2009) Chronosequential changes of selected pedogenic properties in paddy soils as compared with non-paddy soils. *Geoderma* 151:31–41. <https://doi.org/10.1016/j.geoderma.2009.03.016>
- Dauphas N, Janney PE, Mendybaev RA, Wadhwa M, Richter FM, Davis AM, van Zuilen M, Hines R, Foley CN (2004) Chromatographic separation and multicollection-ICPMS analysis of iron. Investigating mass-dependent and -independent isotope effects. *Anal Chem* 76:5855–5863. <https://doi.org/10.1021/ac0497095>
- Dauphas N, John S, Rouxel O (2017) Iron isotope systematics. *Rev Mineral Geochem* 82:415–510. <https://doi.org/10.2138/rmg.2017.82.11>
- Garnier J, Garnier J-M, Vieira CL, Akerman A, Chmeleff J, Ruiz RI, Poitrasson F (2017) Iron isotope fingerprints of redox and biogeochemical cycling in the soil-water-rice plant system of a paddy field. *Sci Total Environ* 574:1622–1632. <https://doi.org/10.1016/j.scitotenv.2016.08.202>
- Guelke M, von Blanckenburg F, Schoenberg R, Staubwasser M, Stuetzel H (2010) Determining the stable Fe isotope signature of plant-available iron in soils. *Chem Geol* 277:269–280. <https://doi.org/10.1016/j.chemgeo.2010.08.010>
- Huang L-M, Jia X-X, Zhang G-L, Thompson A, Huang F, Shao M-A, Cheng L-M (2018) Variations and controls of iron oxides and isotope compositions during paddy soil evolution over a millennial time scale. *Chem Geol* 476:340–351. <https://doi.org/10.1016/j.chemgeo.2017.11.030>
- Ishimaru Y, Suzuki M, Tsukamoto T, Suzuki K, Nakazono M, Kobayashi T, Wada Y, Watanabe S, Matsushashi S, Takahashi M, Nakanishi H, Mori S, Nishizawa NK (2006) Rice plants take up iron as an Fe³⁺-phytosiderophore and as Fe²⁺. *Plant J* 45:335–346. <https://doi.org/10.1111/j.1365-313X.2005.02624.x>
- Johnson CM, Beard BL (2006) Fe isotopes: an emerging technique for understanding modern and ancient biogeochemical cycles. *GSA Today* 16:4–10. <https://doi.org/10.1130/GSAT01611A.1>
- Kalbitz K, Kaiser K, Fiedler S, Kölbl A, Amelung W, Bräuer T, Cao Z, Don A, Grootes P, Jahn R, Schwark L, Vogelsang V, Wissing L, Kögel-Knabner I (2013) The carbon count of 2000 years of rice cultivation. *Glob Chang Biol* 19:1107–1113. <https://doi.org/10.1111/gcb.12080>
- Kirk GJD, Ahmad AR, Nye PH (1990) Coupled diffusion and oxidation of ferrous iron in soils. II. A model of the diffusion and reaction of O₂, Fe²⁺, H⁺ and HCO₃⁻ in soils and a sensitivity analysis of the model. *J Soil Sci* 41:411–431. <https://doi.org/10.1111/j.1365-2389.1990.tb00076.x>
- Kobayashi T, Nishizawa NK (2012) Iron uptake, translocation, and regulation in higher plants. *Annu Rev Plant Biol* 63:131–152. <https://doi.org/10.1146/annurev-arplant-042811-105522>
- Kögel-Knabner I, Amelung W, Cao Z, Fiedler S, Frenzel P, Jahn R, Kalbitz K, Kölbl A, Schloter M (2010) Biogeochemistry of paddy soils. *Geoderma* 157:1–14. <https://doi.org/10.1016/j.geoderma.2010.03.009>
- Kölbl A, Schad P, Jahn R, Amelung W, Bannert A, Cao ZH, Fiedler S, Kalbitz K, Lehndorf M-N, Schloter M, Schwark L, Vogelsang V, Wissing L, Kögel-Knabner I (2014) Accelerated soil formation due to paddy management on marshlands (Zhejiang Province, China). *Geoderma* 228–229:67–89. <https://doi.org/10.1016/j.geoderma.2013.09.005>

- Li Y-L, Vali H, Sears SK, Yang J, Deng B, Zhang CL (2004) Iron reduction and alternation of nontronite N_{Au}-2 by a sulfate-reducing bacterium. *Geochim Cosmochim Acta* 68:3251–3260. <https://doi.org/10.1016/j.gca.2004.03.004>
- Lovley DR, Holmes DE, Nevin KP (2004) Dissimilatory Fe(III) and Mn(IV) reduction. *Adv Microb Physiol* 49:219–286. [https://doi.org/10.1016/S0065-2911\(04\)49005-5](https://doi.org/10.1016/S0065-2911(04)49005-5)
- OriginLab (2019) OriginPro. Version 2019, OriginLab Cooperation, Northampton, MA, USA
- Roth PJ, Lehdorff E, Cao ZH, Zhuang S, Bannert A, Wissing L, Schloter M, Kögel-Knabner I, Amelung W (2011) Accumulation of nitrogen and microbial residues during 2000 years of rice paddy and non-paddy soil development in the Yangtze River Delta, China. *Glob Chang Biol* 17:3405–3417. <https://doi.org/10.1111/j.1365-2486.2011.02500.x>
- Suetsugu A, Sato T, Kaneta Y, Sato A (2005) Effects of organic-mineral complexes on flocculation, settlement and vertical distribution of bioelements in soil suspensions. *Sci Plant Nutr* 51:323–331. <https://doi.org/10.1111/j.1747-0765.2005.tb00037.x>
- Takagi S, Nomoto K, Takemoto T (1984) Physiological aspect of mugineic acid, a possible phytosiderophore of graminaceous plants. *J Plant Nutr* 7:1–5. <https://doi.org/10.1080/01904168409363213>
- Thompson A, Chadwick OA, Rancourt DG, Chorover J (2006) Iron-oxide crystallinity increases during soil redox oscillations. *Geochim Cosmochim Acta* 70:1710–1727. <https://doi.org/10.1016/j.gca.2005.12.005>
- Wang QY (2004) Evolution history of seawall in Cixi County, Zhejiang Province. Fang Zhi Press, Beijing (In Chinese)
- Wang J, Liu ZY (1992) Iron transformation in rice rhizosphere. *Acta Pedol Sin* 29:358–364 (In Chinese)
- Wiederhold JG, Teutsch N, Kraemer SM, Halliday AN, Kretzschmar R (2007) Iron isotope fractionation during pedogenesis in redoximorphic soils. *Soil Sci Soc Am J* 71:1840–1850. <https://doi.org/10.2136/sssaj2006.0379>
- Wiggenhauser M, Moore RET, Wang P, Bienert GP, Laursen KH, Blotevogel S (2022) Stable isotope fractionation of metals and metalloids in plants: a review. *Front Plant Sci* 13:840941. <https://doi.org/10.3389/fpls.2022.840941>
- Wissing L, Kölbl A, Vogelsang V, Fu J-R, Cao Z-H, Kögel-Knabner I (2011) Organic carbon accumulation in a 2000-year chronosequence of paddy soil evolution. *CATENA* 87:376–385. <https://doi.org/10.1016/j.catena.2011.07.007>
- Wissing L, Kölbl A, Schad P, Cao ZH, Kögel-Knabner I (2013) Management-induced organic carbon accumulation in paddy soils: The role of organo-mineral associations. *Soil Tillage Res* 126:60–71. <https://doi.org/10.1016/j.still.2012.08.004>
- Wissing L, Kölbl A, Häusler W, Schad P, Bräuer T, Cao ZH, Kögel-Knabner I (2014) Organic carbon accumulation on soil mineral surfaces in paddy soils derived from tidal wetlands. *Geoderma* 228–229:90–103. <https://doi.org/10.1016/j.geoderma.2013.12.012>
- Wu B, Amelung W, Xing Y, Bol R, Berns AE (2019) Iron cycling and isotope fractionation in terrestrial ecosystems. *Earth-Sci Rev* 190:323–352. <https://doi.org/10.1016/j.earscirev.2018.12.012>
- Zhang GL, Gong ZT (2003) Pedogenic evolution of paddy soils in different soil landscapes. *Geoderma* 115:15–29. [https://doi.org/10.1016/S0016-7061\(03\)00072-7](https://doi.org/10.1016/S0016-7061(03)00072-7)

Publisher's Note Springer Nature remains neutral with regard to jurisdictional claims in published maps and institutional affiliations.